THE JOURNAL OF BIOLOGICAL CHEMISTRY VOL. 285, NO. 9, pp. 6826–6834, February 26, 2010

TDP-43 Is a Developmentally Regulated Protein Essential for Early Embryonic Development*

Received for publication, September 1, 2009, and in revised form, December 24, 2009 Published, JBC Papers in Press, December 29, 2009, DOI 10.1074/jbc.M109.061846

Chantelle F. Sephton[‡], Shannon K. Good[‡], Stan Atkin[§], Colleen M. Dewey[‡], Paul Mayer III[‡], Joachim Herz[¶], and Gang Yu[‡1]

From the Departments of [‡]Neuroscience, [¶]Molecular Genetics, and [§]Pharmacology, University of Texas Southwestern Medical Center, Dallas, Texas 75390

TDP-43 is a DNA/RNA-binding protein implicated in multiple steps of transcriptional and post-transcriptional regulation of gene expression. Alteration of this multifunctional protein is associated with a number of neurodegenerative diseases including amyotrophic lateral sclerosis and frontotemporal lobar degeneration with ubiquitin positive inclusions. Whereas a pathological link to neurodegenerative disorders has been established, the cellular and physiological functions of TDP-43 remain unknown. In this study, we show that TDP-43 is a nuclear protein with persistent high-level expression during embryonic development and with progressively decreased protein levels during postnatal development. In mice where the TDP-43 gene (*Tardbp*) was disrupted using a gene trap that carries a β-galactosidase marker gene, heterozygous (*Tardbp*$^{+/-}$) mice are fertile and healthy, but intercrosses of *Tardbp*$^{+/-}$ mice yielded no viable homozygotic null (*Tardbp*$^{-/-}$) mice. Indeed, *Tardbp*$^{-/-}$ embryos die between 3.5 and 8.5 days of development. *Tardbp*$^{-/-}$ blastocysts grown in cell culture display abnormal expansion of their inner cell mass. The pattern of β-galactosidase staining at E9.5 *Tardbp*$^{+/-}$ embryos is predominantly restricted to the neuroepithelium and remains prominent in neural progenitors at E10.5–12.5. TDP-43 is detected in spinal cord progenitors and in differentiated motor neurons as well as in the dorsal root ganglia at E12.5. β-Galactosidase staining of tissues from adult *Tardbp*$^{+/-}$ mice shows widespread expression of TDP-43, including prominent levels in various regions of the central nervous system afflicted in neurodegenerative disorders. These results indicate that TDP-43 is developmentally regulated and indispensible for early embryonic development.

The gene coding TDP-43,[2] or TAR DNA-binding protein 43 (*Tardbp*), is highly conserved throughout evolution and is found in all higher eukaryotic species including distant species *Drosophila melanogaster*, *Xenopus laevis*, and *Caenorhabditis elegans* (1, 2). In humans, *Tardbp* is located at the chromosomal locus 1p36.22 and is comprised of six exons, five of which encode a ubiquitously expressed, predominantly nuclear, 43-kDa protein that contains two RNA recognition motifs and a glycine-rich C-terminal domain, characteristic of the heterogeneous nuclear ribonucleoprotein class of proteins (3). The RNA recognition motif domains of TDP-43 are highly homologous among species; however, the glycine-rich sequence varies significantly among all species, reflecting species-specific functions in the different organisms.

TDP-43 has been implicated in the regulation of gene transcription, pre-mRNA splicing, mRNA stability, and mRNA transport (4). It was first identified to bind the TAR DNA of the human immunodeficiency virus 1 long terminal repeat region. Both *in vitro* and *in vivo* experiments showed that TDP-43 represses human immunodeficiency virus 1 proviral gene expression (5). Later, it was shown to enhance exon skipping of the cystic fibrosis transmembrane conductance regulator exon 9 through binding to a $(UG)_m(U)_n$ motif near the 3′ splice site of the cystic fibrosis transmembrane conductance regulator intron 8 (6). TDP-43 was also shown to be involved in splicing of the apolipoprotein A-II (7) and survival of motor neuron (8) genes. In addition, TDP-43 has been implicated in regulation of mRNA biogenesis (9) and shown to be localized to sites of mRNA transcription and processing in neurons (10). As the glycine-rich domain of TDP-43 has been shown to mediate interactions with other heterogeneous nuclear ribonucleoprotein proteins, the low homology of this particular domain may afford a multitude of interactions that allows for diverse biological functions (11).

TDP-43 has been identified as the primary protein of neuronal and glial inclusions of sporadic and familial frontotemporal lobar degeneration with ubiquitin positive inclusions (FTLD-U), as well as in sporadic and the majority of familial amyotrophic lateral sclerosis (ALS) cases (12, 13). TDP-43, normally observed in the nucleus, is found in pathological inclusions mostly in the cytoplasm and in some cases accumulates in dense deposits in the nucleus. The inclusions consist prominently of TDP-43 C-terminal fragments of ~20–25 kDa. Both full-length and C-terminal fragments of TDP-43 undergo abnormal phosphorylation and ubiquitination in diseased states (13). More recently, TDP-43 inclusions are found in patients with Alzheimer and Parkinson diseases implying a common mechanism of TDP-43-related

* This work was supported, in whole or in part, by National Institutes of Health Grants R01 AG029547 and AG023104, Welch Foundation Grant I-1566, the Ted Nash Longlife Foundation, and the Consortium for Frontotemporal Dementia Research.

[1] To whom correspondence should be addressed: 6000 Harry Hines Blvd., Dallas, TX 75390-9111. Tel.: 214-648-5157; Fax: 214-648-1801; E-mail: Gang.Yu@UTSouthwestern.edu.

[2] The abbreviations used are: TDP-43 or *Tardbp*, TAR DNA-binding protein; ALS, amyotrophic lateral sclerosis; FTLD-U, frontotemporal lobar degeneration with ubiquitin positive inclusions; dpc, days post coitus; ES, embryonic stem; X-gal, 5-bromo-4-chloro-3-indolyl-β-D-galactopyranoside; ICM, inner cell mass; WT, wild type; PFA, paraformaldehyde; PBS, phosphate-buffered saline.

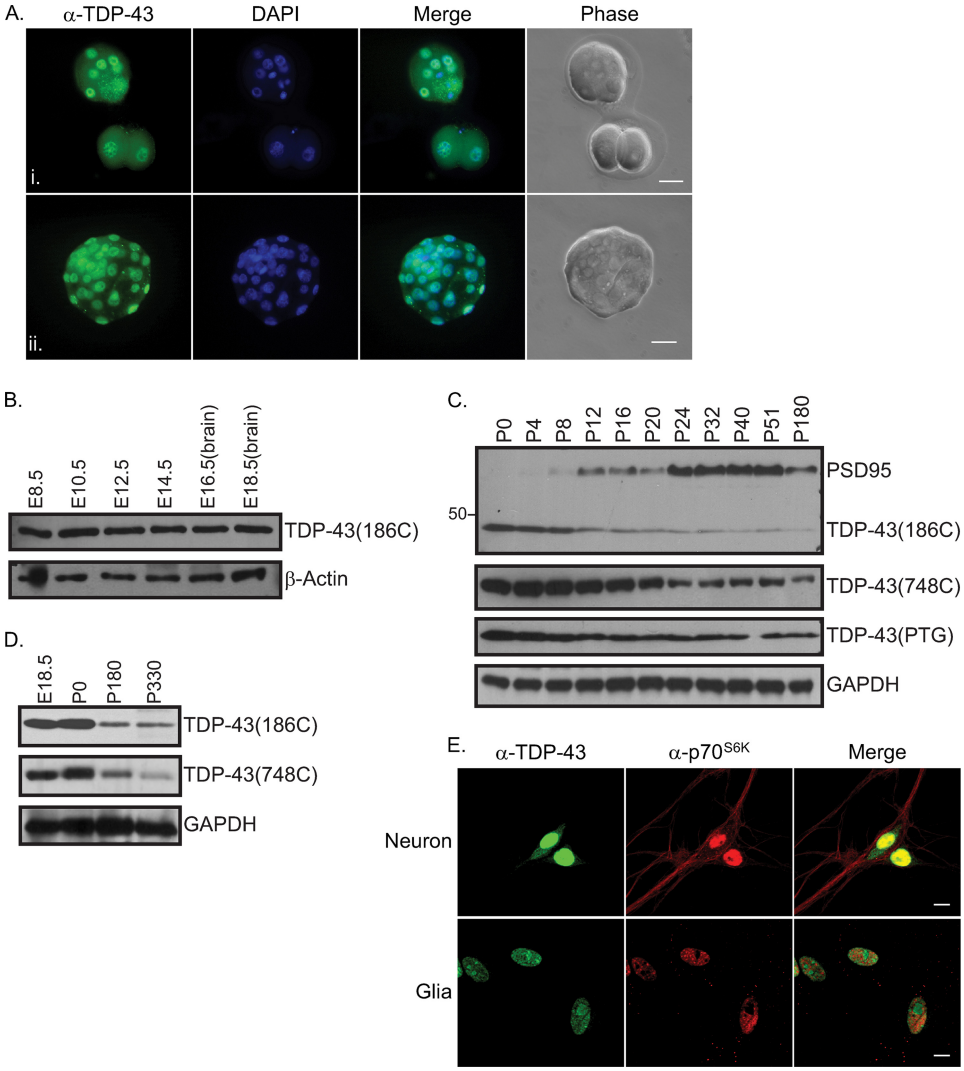

FIGURE 1. **Expression of TDP-43 during development.** *A*, embryos (*i*), two- and six-cell stage, and (*ii*) blastocyst stage, E3.5, were harvested from superovulated female WT mice from intercrossed mating. Embryos were incubated with anti-TDP-43(PTG), followed by Alexa Fluor 488 (*green*) and stained with 4′,6-diamidino-2-phenylindole (*DAPI*) (*blue*). *Scale bars* represent 100 μm. *B–D*, whole embryos (E8.5–14.5) and the brains from embryos (E16.5 and E18.5) and postnatal mice were harvested at the indicated times and proteins were extracted. *B*, Western blot showing protein expression of TDP-43 in the developing embryo using anti-TDP-43 (186C). Levels of β-Actin were used as a loading control. *C*, Western blot of brain lysates from postnatal mice probed with anti-TDP-43(186C), anti-TDP-43(748C), commercially available anti-TDP-43(PTG) and anti-PSD95. *D*, Western blot of brain lysates from E18.5, P0, P180, and P330 using anti-TDP-43(186C) and TDP-43(748C). Levels of glyceraldehyde-3-phosphate dehydrogenase (*GAPDH*) were used as a loading control. *E*, mouse primary cortical neurons and glia stained with anti-TDP-43(PTG) and anti-p70^{S6K}, followed by Alexa Fluor 488 (*green*) and Alexa Fluor 546 (*red*). *Scale bars* represent 10 μm.

pathologies (14, 15). The relevance of TDP-43 and its pathological function was supported by the discovery of autosomal dominant mutations in *Tardbp* in patients with familial and sporadic ALS (16, 17). Most of these mutations are found in the C-terminal region of TDP-43, supporting an important function of this region and involvement of the C-terminal derivatives in disease onset and progression (18, 19). Furthermore, mice overexpressing the familial A315T mutation of TDP-43 result in ubiquitin aggregates with degeneration of cortical projection neurons and spinal motor neurons similar to that observed in ALS and FTLD-U (20). Alternatively, a loss of TDP-43 function rather than the production of C-terminal fragments may lead to TDP-43-associated pathologies. It has been reported that TDP-43-null flies display deficient locomotor behavior and have reduced life span and defects at the neuromuscular junction (21). Knockdown of TDP-43 by small interfering RNA in cellular models reveals disruption of cell proliferation (22), inhibition of differentiation, and neuronal cell death (23).

Whereas a pathological link to neurodegenerative disorders has been established, the cellular and physiological functions of TDP-43 remain unknown. As a first step toward the elucidation of the fundamental role of TDP-43 *in vivo*, we disrupted the *Tardbp* gene in mice and found that TDP-43 is necessary for embryonic development: no *Tardbp*$^{-/-}$ embryos survived after 3.5 days post coitus (dpc), whereas *Tardbp*$^{+/-}$ mice were healthy and indistinguishable from their control littermates. We also found that TDP-43 is present throughout embryonic development and is expressed predominantly in the neuroepithelium and neural progenitors of the developing embryo. We show nuclear expression of TDP-43 in embryonic stem (ES) cell outgrowths and in hippocampal neurons and glia. Moreover, we observed in postnatal brains that TDP-43 holoprotein is developmentally regulated. In adult mice, TDP-43 shows widespread expression, including prominent levels in various regions of the central nervous system afflicted in neurodegenerative disorders.

EXPERIMENTAL PROCEDURES

Materials—Restriction enzymes were from New England Biolabs, Inc. Electrophoresis reagents were from Bio-Rad. All other reagents and chemicals were reagent grade. TDP-43 was detected with the 186C antibody generated against the full-length mouse TDP-43 recombinant protein produced in bacteria using TDP-43-His$_6$ cloned into pET28a+ (Invitrogen) and with peptide antibodies 748C (NQGNMQREPNQAFGSGNN) and 750C (RVTEDENDEPIEIPSEDDG). Other antibodies include: TDP-43 (Proteintech Group Inc. (PTG)); glyceraldehyde-3-phosphate dehydrogenase, β-galactosidase and β-actin (Sigma); PSD95 (ABR Affinity Bioreagents); p70^{S6K} (Santa Cruz); VCP (a gift from T. C. Sudhof (24)); anti-rabbit [^{125}I] (PerkinElmer); and Alexa^{TM} 488-conjugated anti-rabbit IgG and Alexa^{TM} 546-conjugated anti-mouse IgG (Molecular Probes).

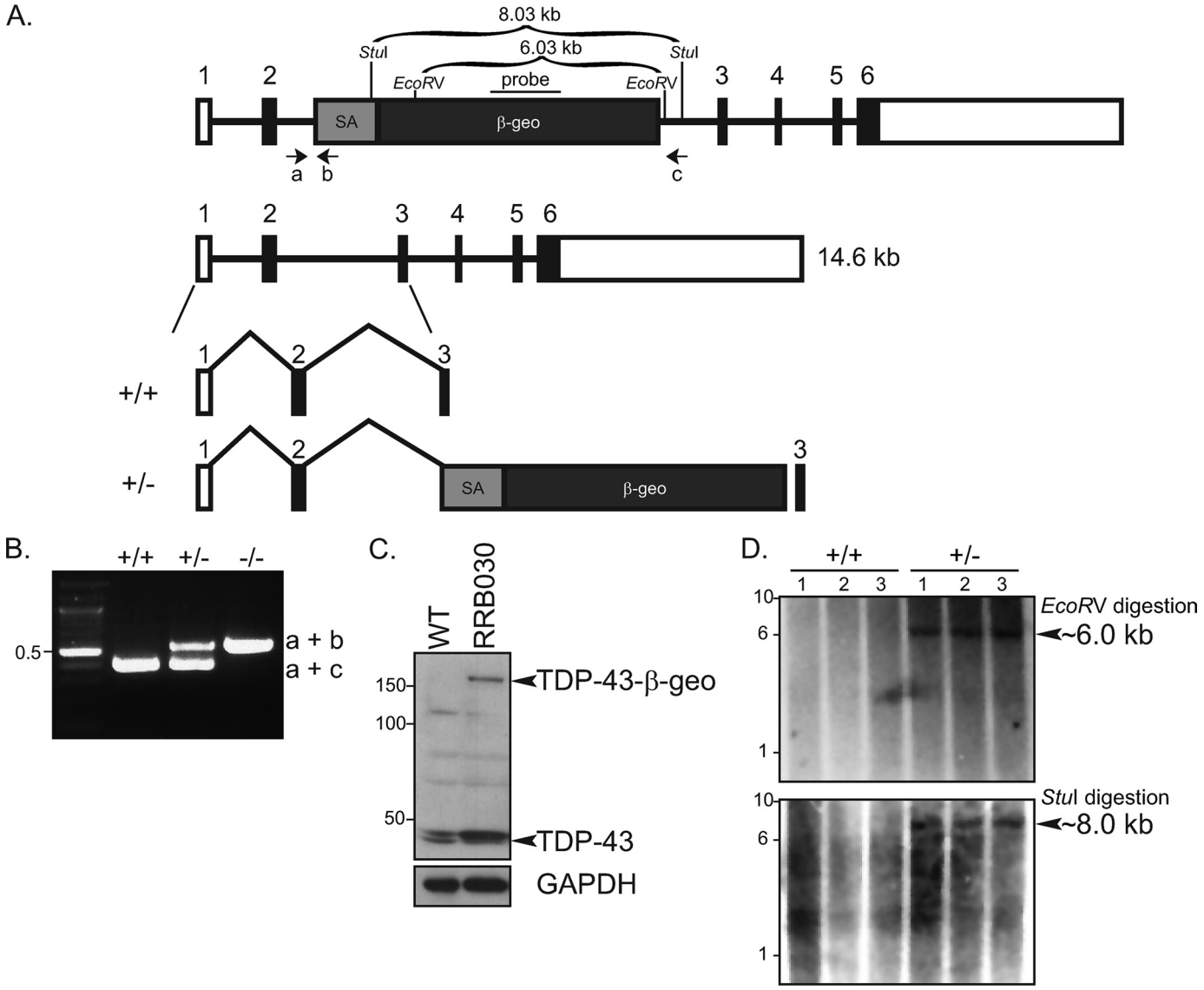

E.

Genotypes of offspring from *Tardbp* heterozygous intercrosses

Line:	+/+ (M:F)	+/- (M:F)	-/- (M:F)	Total
RRB030	43:29 (33%)	67:77 (67%)	0:0 (0%)	216

FIGURE 2. **Generation of TDP-43 knock-out mouse.** *A*, schematic of the gene trap in *Tardbp*. *Numbered boxes* represent exons. The mutated allele yields an in-frame fusion transcript with exons 1–2 of *Tardbp* and β-geo. Oligonucleotide primers a, b, and c are indicated. *SA*, splice acceptor. *B*, genotyping of E3.5 embryos by PCR. *C*, Western blot showing expression of the WT TDP-43 protein in ES cells and expression of the TDP-43-β-geo fusion protein in targeted ES cells using an N-terminal TDP-43 (750C) antibody. Glyceraldehyde-3-phosphate dehydrogenase (*GAPDH*) was used as a loading control. *D*, identification of a single gene trap insertion using Southern blot. Genomic DNA was digested with EcoRV or StuI and hybridized with a ^{32}P-labeled neomycin phosphotransferase II probe and the predicted ~6- or ~8-kb band, respectively, was detected in *Tardbp*$^{+/-}$ mice only. *E*, genotyping results of offspring from intercrossed *Tardbp*$^{+/-}$ mice.

Generation of TDP-43 Knock-out Mice—Mouse ES cell lines (RRB030, YBH106, and YDH133; strain 129P2) with insertional mutation in *Tardbp* were purchased from BayGenomics. The gene trap vector, pGT1Lxf, creates an in-frame fusion between the 5′ exons of the trapped gene and a β-geo reporter. The ES cells were injected into C57BL/6 blastocysts to create chimeric mice, which were bred with C57BL/6 mice to generate heterozygous (+/−) *Tardbp*-deficient mice. The RRB030 line was further analyzed in this study. The YBH106 and YDH133 lines were not pursued as these ES cells did not yield workable animals.

Genotyping—Genomic DNA from ear biopsies, yolk sacs, and embryos were lysed in Quick Lysis Buffer (50 mM NaCl, 10 mM Tris-HCl, pH 8.3, 0.2% Tween 20, 0.4 mg/ml of proteinase K) at 55 °C for 1 h and then 95 °C for 10 min. The PCR contained primer-a (5′-GCTGGGTCTGTGGTGCACGTC-3′) and prim-

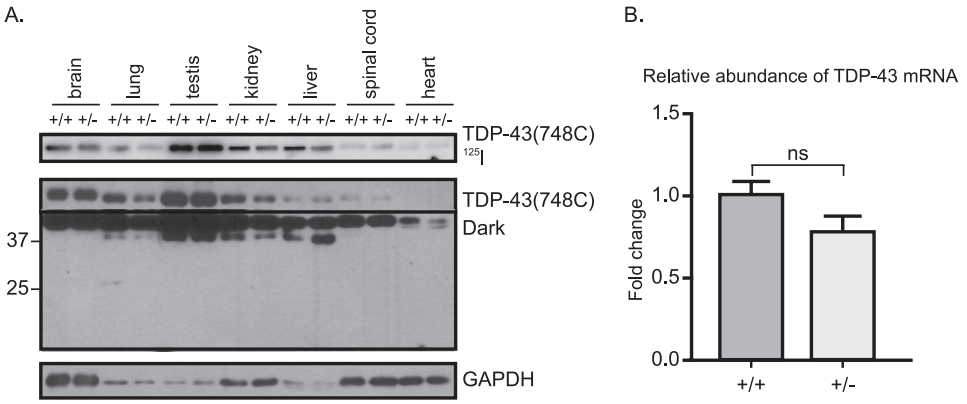

FIGURE 3. **Expression profile of TDP-43 in *Tardbp*$^{+/-}$ mice.** *A*, Western blot showing protein expression of TDP-43 in *Tardbp*$^{+/-}$ and WT (*Tardbp*$^{+/+}$) mice using the C-terminal TDP-43(748C) antibody and enhanced chemiluminescence (*lower panels*) or ^{125}I-labeled anti-rabbit secondary antibody (*upper panel*). *B*, quantitative PCR analysis of TDP43 mRNA levels in WT and heterozygous mice using the comparative threshold cycle method relative to U36B as an internal control. Data were analyzed by unpaired Student's *t* test and are represented as relative to WT mRNA ($n = 3$; *ns*, not significant). *Error bars* represent the mean ± S.E.

A.

Genotypes of embryos from *Tardbp* heterozygous intercrosses

RRB030:	+/+	+/-	-/-	Total
E12.5	4	10	0	14
E9.5	13	33	0	46
E8.5	4	10	0	14
E3.5	11	25	11	47

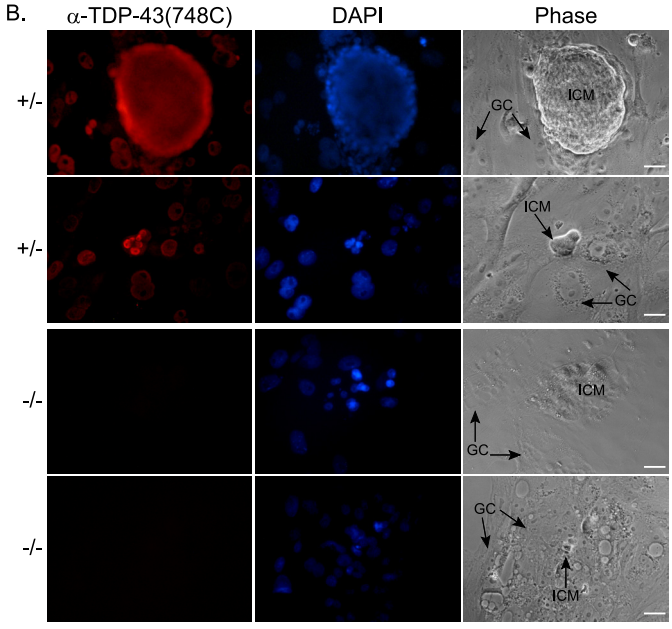

FIGURE 4. **TDP-43 is necessary for expansion of the inner cell mass.** *A*, genotyping results of embryos collected at 12.5, 9.5, 8.5, and 3.5 dpc from intercrossed *Tardbp*$^{+/-}$ mice. *B*, blastocysts at E3.5 were grown *in vitro* for 7 days. Outgrowths were incubated with anti-TDP-43(748C), followed by Alexa Fluor 546 (*red*). Nuclei were stained with 4′,6-diamidino-2-phenylindole (*DAPI*) (*blue*). WT and heterozygous embryos displayed expansion of the ICM and giant trophoblasts (*GC*), whereas homozygous embryos had no ICM expansion. *Scale bars* represent 100 μm.

er-c (5′-GCTCATGCTCCTGTCTCCCTCCTTC-3′), which correspond to sequences upstream and downstream, respectively, of the insertion point and primer-b (5′-GTACCGCACTGCCG-GTTTCCTCCACC-3′), which is specific to pGT1LxF. Genomic DNA (100 ng) and primers-a, -b, and -c (300 nM each) were placed in standard *Taq* buffer supplemented with 1 M betaine, 3.3% dimethyl sulfoxide, 1.5 mM $MgCl_2$, 0.1 mg/ml of bovine serum albumin, 0.2 mM deoxynucleoside triphosphates, and 1.25 units of *Taq* polymerase (New England Biolabs) for 10 min at 94 °C. After enzymatic amplification for 35 cycles, the PCR products were resolved on 2% agarose gel in 1× Tris acetate-EDTA buffer. Primers-a and -b amplify a 600-bp band from mutant allele; primers-a and -c amplify a 400-bp band from the wild-type (WT) allele.

Southern Blot—Genomic DNA was purified from 6-week-old mice (F4 generation), digested overnight with EcoRV or StuI, and analyzed by Southern blot with a ^{32}P-labeled neomycin phosphotransferase II probe.

LacZ Staining of Tissues and Embryos—Mice were anesthetized with avertin and perfusion-fixed with 4% paraformaldehyde (PFA). Tissues were harvested and post-fixed in 4% PFA overnight at 4 °C, washed with PBS, immersed in 30% sucrose for 24 h at 4 °C, and frozen in optimal cutting temperature compound for sectioning. β-Galactosidase activity was assessed by incubating 30–50-μm thick sections with LacZ staining solution (1.0 mg/ml of X-gal (Invitrogen), 5 mM potassium ferrocyanide, 5 mM potassium ferricyanide, 2 mM $MgCl_2$) for 24 h at 37 °C and fixed in 4% PFA. After counterstaining with nuclear fast red, the sections were examined and photographed with a Zeiss SteREO Discovery version 12 microscope.

Whole embryos were harvested and post-fixed in LacZ fixing solution (1% PFA, 0.2% glutaraldehyde, 2 mM $MgCl_2$, 5 mM EGTA, pH 8.0) for 15 min at room temperature, washed with PBS containing 2 mM $MgCl_2$, and incubated in LacZ staining solution for 30 min. Embryos were then post-fixed with 4% PFA for 30 min, immersed in 30% sucrose for 24 h at 4 °C, and frozen in optimal cutting temperature compound for sectioning.

Western Blot and Quantification of Proteins Using ^{125}I—Total proteins were extracted using ice-cold lysis buffer (50 mM HEPES, pH 7.5, 4 M urea, 1% lithium dodecyl sulfate, 1 mM sodium fluoride, 1 mM sodium orthovanadate, 1× protease inhibitors (Roche), 1 mM phenylmethylsulfonyl fluoride). Lysates were sonicated and precleared by centrifugation. Total lysates were resolved by SDS-PAGE and transferred to polyvinylidene difluoride membranes (Millipore Corp.). Membranes were probed overnight (4 °C) and protein detection relied on enhanced chemiluminescence.

For ^{125}I quantification of proteins, proteins were processed as described above, transferred to a polyvinylidene difluoride membrane, and blocked in 5% milk and 5% goat serum for 1 h at room temperature. Membranes were then incubated with primary antibodies TDP-43 (748C) (1:1000) and VCP (1:500) over-

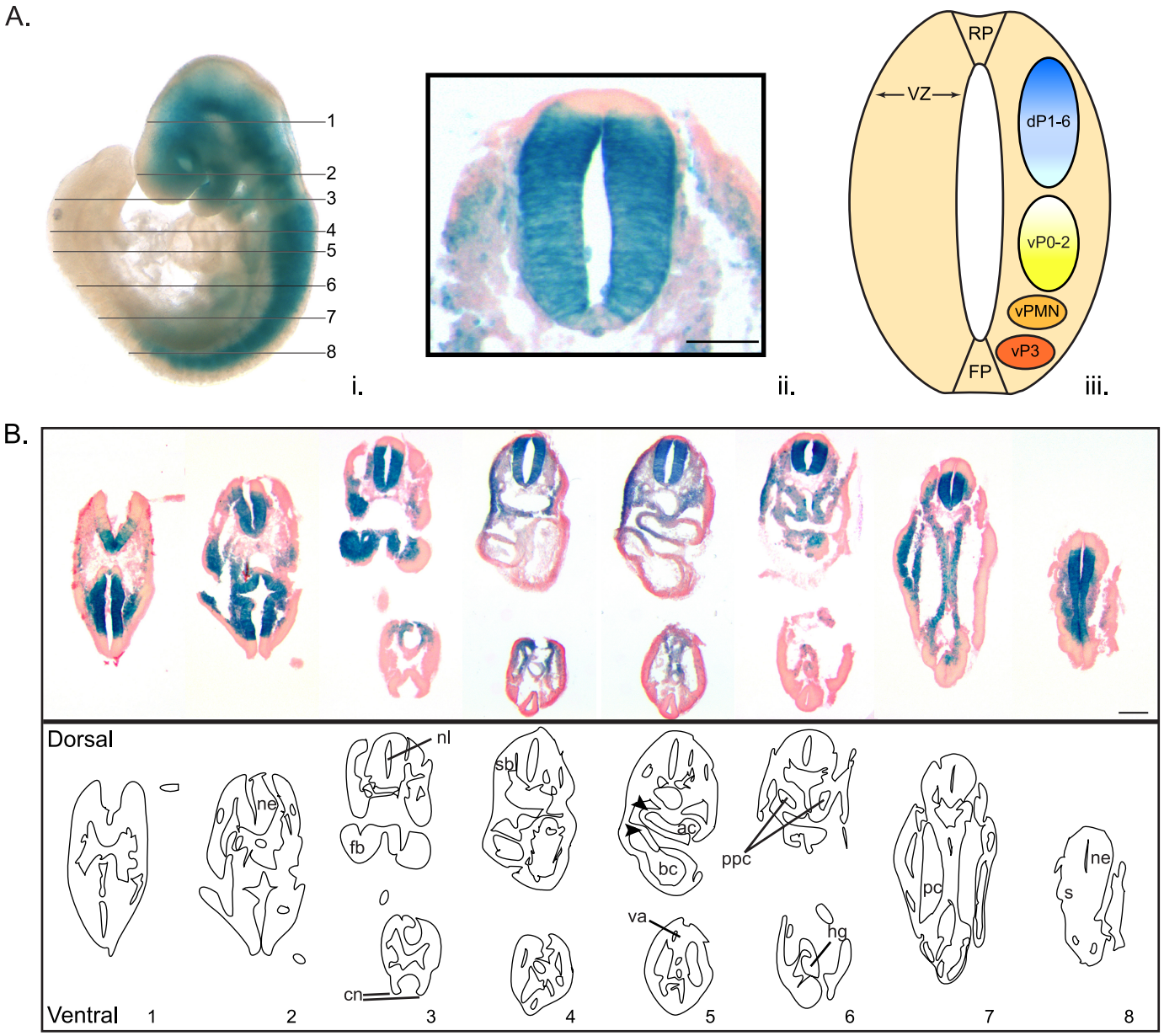

FIGURE 5. **TDP-43 expression in the developing mouse embryo.** β-Galactosidase staining of a *Tardbp*$^{+/-}$ embryo at E9.5. *A* (*i*), whole mount embryo, *numbers* indicate corresponding sections shown in 5*B*. (*ii*) Transverse section counterstained with nuclear fast red showing X-gal staining in the neuroepithelium of the neural tube. *Scale bar* represents 100 μm. (*iii*) Schematic of neuroepithelium indicating the domains for neuronal progenitors. Dorsal progenitors (*dP*) are indicated as dP1–6. Ventral progenitors (*vP*) vP0-p3 give rise to interneurons subtypes, vPMN is the source of motor neurons. The floor plate position (*FP*), an important source of Shh proteins, and the roof plate (*RP*), a source of bone morphogenetic proteins, are shown (adapted from Refs. 30 and 31). *B*, transverse sections of whole embryo in series. There is strong staining in the neuroepithelium (*ne*) of the neural tube and to a lesser extend the first branchial arch (*fb*), second branchial membrane (*sb*), atrial heart chamber (*ac*), vitelline artery (*va*), bulbus cordis heart region (*bc*), left and right pericardio-peritoneal canal (*ppc*), hindgut (*hg*), and somite (*s*). Also annotated are the neural folds in caudal neuropore (*cn*), neural lumen (*nl*), and peritoneal cavity (*pc*). The developing heart is indicated by *arrows*. *Scale bars* represent 200 μm.

night at 4 °C, and then at room temperature for 2 h. Membranes were washed 3 times for 30 min with Tris-buffered saline-Tween 20 (TBS-T), followed by incubation with ^{125}I-labeled anti-rabbit IgG (1:1000) diluted in 5% milk/TBS-T with 0.05% NaN_3 and incubated overnight. The blots were washed 5 times for 5 min with TBS-T and exposed to a phosphorimager screen for 3 days before analysis.

Quantitative PCR Analysis—Primers were designed using Primer Express software (Applied Biosystems) based on GenBank™ sequence data. Primer sequences were BLASTed against the NCBI mouse genomic sequence data base to ensure unique specificity. Primer sequences for TDP-43 include 5′-CGTGTCTCAGTGTATGAGAGGAGTC-3 and 5′-CTGCAGAGGAAGCATCTGTCTCATCC-3′. Reverse transcription quantitative-PCR (10 μl) contained 20 ng of cDNA, 150 nM of each primer, and 5 μl of SYBR FastGreen PCR Master Mix (Applied Biosystems). All reactions were performed in triplicate on an Applied Biosystems Prism 7500Fast sequence detection system, and relative mRNA levels were calculated by the comparative threshold cycle method using U36B primers (5′-TGGGCATCACCACGAAAAT-3′ and 5′-TATCAGCTGCACATCACTCAGAATT-3′) as the internal controls.

Primary Neuronal and Glial Cultures—Cultures were generated by adapting previously established protocols (25, 26). Briefly, hippocampi and neocortex were dissected from E18 and P1 mouse brains, respectively. Hippocampal neurons were dissociated with papain (20 units/ml) for 4 min at 37 °C, triturated with a Pasteur pipette, and plated at 1×10^5 cells/cm^2 onto nitric acid-etched coverslips coated with poly-D-lysine and Matrigel (BD Biosciences). Cultures were maintained for 21 days *in vitro* in Neuroblasal medium supplemented with 2% B27 (Invitrogen) and 1% L-glutamine (Sigma). Neocortex-derived glia were dissociated with papain for 15 min at 37 °C, triturated, and plated onto poly-D-lysine-coated 10-cm plates. Glia were maintained for 30 days *in vitro* in Dulbecco's modified Eagle's medium, 10% fetal bovine serum (Invitrogen), and 5% L-glutamine. Cells were incubated with anti-TDP-43 (1:200) and anti-p70^{S6K} (1:500), followed by incubation with Alexa 488-conjugated anti-rabbit IgG and Alexa 546-conjugated anti-mouse IgG (1:500), respectively. Images were captured using a Zeiss 510 confocal microscope; images were processed using LSM software.

Analysis of Tardbp-deficient ES Cells—Female *Tardbp*$^{+/-}$ mice were superovulated by injection with 7 units of pregnant mare serum gonadotropin, followed 48 h later by injection of 7 units of human chorinonic gonadotropin and then mated with stud male *Tardbp*$^{+/-}$ mice. Fertilized eggs were collected 3.5 days post-impregnation and genotyped as described above or placed in 12-well cell culture dishes containing coverslips coated with 0.1% gelatin. Blastocysts were cultured for 7 days in ES cell medium (knock-out Dulbecco's modified Eagle's medium supplemented with 15% fetal bovine serum, penicillin (100 units/ml)/streptomycin, 2 mM L-glutamine, 1× minimal essential medium non-essential amino acids, 100 mM β-mercaptoethanol).

After 7 days the ES cell outgrowths were fixed in 4% PFA for 30 min, washed twice in PBS containing 1% goat serum, followed by permeabilization in PBS containing 0.2% Triton X-100 for 15 min. Cells were washed twice in PBS containing 1% goat serum, blocked with 10% goat serum and 0.1% Triton X-100, and incubated with anti-TDP-43(748C) antibody (1:500) for 1 h at room temperature. Cells were then incubated with Alexa 546-conjugated anti-mouse IgG (1:500), followed by 4′,6-diamidino-2-phenylindole staining. Samples were analyzed using a Nikon Eclipse TS100 fluorescence microscope.

RESULTS AND DISCUSSION

TDP-43 Protein Is Developmentally Regulated—Proteins relevant to central nervous system disease pathogenesis, for example, the Alzheimer disease-associated amyloid precursor protein (27), are often developmentally regulated or play important developmental roles. Taking cues from this observation, we examined subcellular localization and protein levels of the TDP-43 protein in developing embryos and postnatal brains of WT mice. Embryos harvested at the two- and six-cell stage (Fig. 1*A*, *panel i*) and at the blastocyst stage (E3.5, Fig. 1*A*, *panel ii*) from intercrossed WT mice were immunoreactive for the TDP-43 protein. At these stages of development TDP-43 was confined to the nucleus of cells. The level of TDP-43 holoprotein was maintained in the developing embryos (Fig. 1*B*), but in

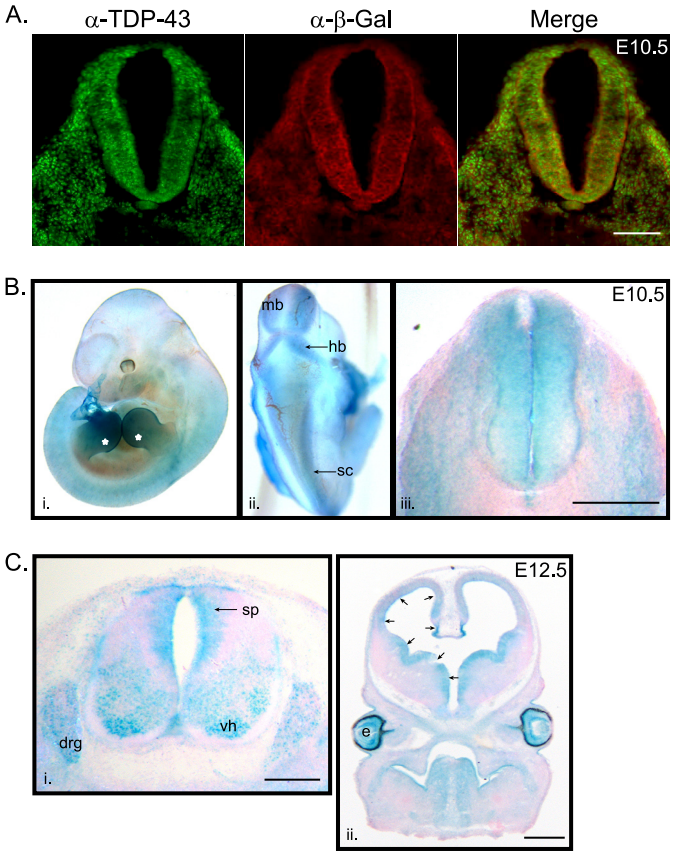

FIGURE 6. **TDP-43 expression in spinal cord and telencephalon progenitor cells.** *A*, cross-section of *Tardbp*$^{+/-}$ spinal cord showing TDP-43 and β-galactosidase immunostaining at E10.5. *B*, X-gal staining of a *Tardbp*$^{+/-}$ embryo at E10.5. (*i*) Whole mount embryo, *asterisks* indicate developing limbs. (*ii*) Dorsal view, showing staining in spinal cord (*sc*), midbrain (*mb*), and hindbrain (*hb*). (*iii*) Transverse sections of spinal cord showing X-gal staining in the neuroepithelium. *C* (*i*), transverse sections of spinal cord of *Tardbp*$^{+/-}$ at E12.5 showing X-gal staining in spinal cord progenitors (*sp*), dorsal root ganglia (*drg*), and in motor neurons of the ventral horn (*vh*) and (*ii*) coronal section of the developing brain showing prominent X-gal staining in progenitors (indicated by *arrows*) and eye (*e*). X-gal-stained sections were all counterstained with nuclear fast red. *Scale bars* for *A*, *B*, and *Ci* represent 10 μm and for *Cii*, 200 μm.

postnatal brains the expression gradually decreased after birth (Fig. 1, *C* and *D*). The progressive postnatal decrease of TDP-43 protein does not result from reduced mRNA transcripts. mRNA levels stay relatively constant in the late embryonic stages and several days after birth, then modestly increase in the adult brains (data not shown). Co-staining of hippocampal neurons and glia from mice with anti-TDP-43 and anti-p70^{S6K}, a duo-specific nuclear and processing body marker (28), show nuclear staining of TDP-43 (Fig. 1*E*).

TDP-43 Is Required for Early Embryogenesis—Having observed that TDP-43 is a developmentally regulated protein, we next determined the developmental and physiological function of TDP-43 in mice wherein *Tardbp* was disrupted using a gene trap (Fig. 2*A*). The gene trap vector, pGT1Lxf, creates an in-frame fusion between the 5′ exons of the trapped gene and a β-geo (a fusion of β-galactosidase and neomycin phosphotransferase II) reporter gene. The insertional mutation in the RRB030 *Tardbp*$^{+/-}$ mice was located within intron-2 of *Tardbp* and a genotyping approach was established (Fig. 2*B*). The insertional mutation, which is predicted to generate a fusion

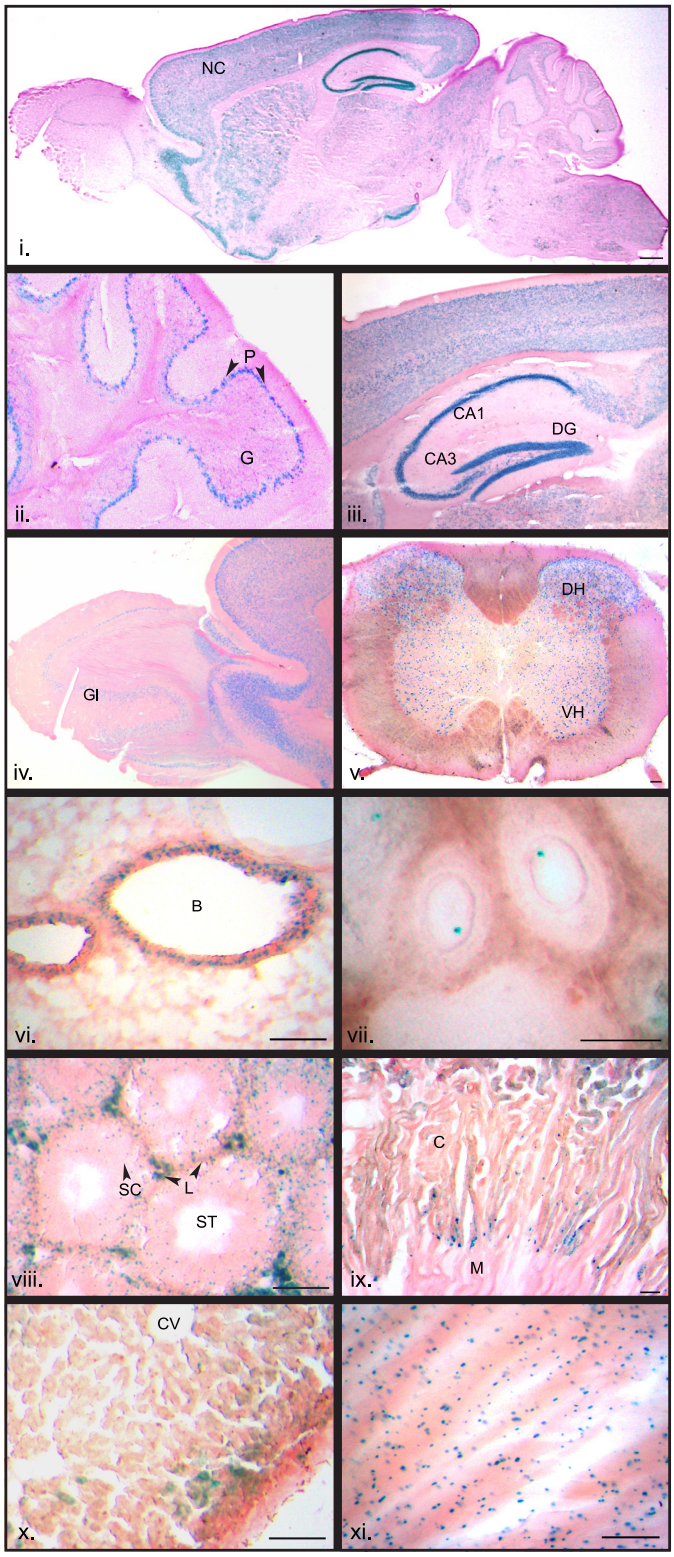

FIGURE 7. **TDP-43 expression in adult tissues.** β-Galactosidase expression in adult *Tardbp*$^{+/-}$ mice was observed in (*i*) whole brain with prominent staining in the neocortex (*NC*), (*ii*) cerebellar cortex staining in the granular cell layer (*G*) and Purkinje cells (*P*), and (*iii*) in the hippocampus (shown are granular dentate gyrus (*DG*) as well as CA1 and CA3 regions). There is also distinct staining in the (*iv*) olfactory bulb glomerulus (*GI*). Staining is observed throughout the (*v*) spinal cord mostly in the dorsal horn (*DH*) and to a lesser extent the ventral horn (*VH*). Staining is in the bronchiole (*B*) region of the (*vi*) lung and throughout the (*vii*) ovary, particularly in the oocytes, as well as in the (*viii*) testis, at the periphery of the seminiferous tubules (*ST*) where Sertoli cells (*SC*) are found and with some interstitial staining of Leydig (*L*) cells. Staining in (*ix*) kidney is concentrated in the (*C*) cortical region (shown is the medulla (*M*)). Moderate levels of expression were in the (*x*) liver (shown is the central vein (*CV*)) and (*xi*) heart. *Scale bars* represent 100 μm.

transcript containing exons 1–2 of *Tardbp* and β-geo, was detected around ~175 kDa in the *Tardbp*$^{+/-}$ targeted ES cell line (Fig. 2*C*). The fusion protein contains the first 79 translated amino acids of TDP-43, which is not predicted to produce a functional protein. Southern blot analysis shows a ~6 or ~8 kb band from genomic DNA digested with EcoRI or StuI, respectively, in heterozygous mice only, indicating no additional genes are trapped in these mice (Fig. 2*D*).

Tardbp$^{+/-}$ mice were indistinguishable from their control littermates; heterozygotes had normal body weight, growth rate, appearance, and fertility (data not shown), and there were no premature postnatal deaths in these mice (Fig. 2*E*). Furthermore, there were no gross tissue abnormalities in any tissue observed, including the brain, spinal cord, lung, ovaries, testis, kidney, heart, and liver up to 6 months of age (see Fig. 7). Quantitative assessment of the protein levels of TDP-43 in tissues from *Tardbp*$^{+/-}$ mice using ^{125}I-labeled secondary antibody and densitometry showed that TDP-43 levels were unchanged between heterozygous and WT mice (Fig. 3*A* and data not shown). Analysis of mRNA showed no significant decrease in TDP-43 mRNA in brain (Fig. 3*B*, $n = 3$) and other tissues including testis, liver, heart, spinal cord, and lung of *Tardbp*$^{+/-}$ mice (data not shown). The lack of changes in mRNA and protein levels suggests a compensatory mechanism, perhaps by increased TDP-43 mRNA stability or by an increased rate of transcription from the WT allele, or by post-translational regulation. The compensated levels of TDP-43 may explain why the *Tardbp*$^{+/-}$ mice do not display any overt phenotype.

Mice heterozygous for the non-functional *Tardbp* allele were intercrossed, but no homozygous mice were identified of 216 pups born, suggesting embryonic lethality (Fig. 2*E*). Therefore, embryos were genotyped at different time points during development to determine the stage of lethality. At 8.5, 9.5, and 12.5 dpc no *Tardbp*$^{-/-}$ embryos survived (Fig. 4*A*). However, genotyping of blastocysts at 3.5 dpc revealed that *Tardbp*$^{-/-}$ embryos were present at the expected Mendelian frequency (Fig. 4*A*) and microscopy revealed normal morphology (data not shown). These results indicate *Tardbp*$^{-/-}$ embryos die between day 3.5 and 8.5 post-fertilization, implying no functional redundancy of TDP-43 with other proteins, including other heterogeneous nuclear ribonucleoproteins. Death of *Tardbp*$^{-/-}$ embryos suggests that TDP-43 may be essential for transcription or mRNA splicing or processing, all of which are critical for developmental stages of implantation, gastrulation, and early organogenesis.

To identify the effect of the *Tardbp* null mutation in ES cell development, blastocysts from heterozygous intercrossed mice were harvested at E3.5 and cultured *in vitro* for 7 days. Heterozygous and WT embryos grew at similar rates, attaching to the coverslip after 2 days, subsequently expanding their inner cell mass (ICM) and growing as a mound on top of the trophoblast giant cells (Fig. 4*B*). The expanded ICM of the heterozygous and WT embryos were all immunoreactive for TDP-43

(Fig. 4*B*). Homozygous embryos showed signs of aberrant development: these embryos attached to the coverslip, but their ICM did not expand leaving behind a monolayer of giant cells with large nuclei (Fig. 4*B*). These data suggest that *Tardbp*-null embryos experience developmental defects due to lack of ICM expansion prior to implantation. An independent study recently reported a similar defect in ICM expansion of TDP-43 knock-out embryos (29). Feiguin *et al.* (21) demonstrated that *D. melanogaster* lacking TDP-43 display deficits in locomotor behavior and have reduced lifespan. Although mouse and fly display high homology in the RNA recognition motif domains, the C-terminal region has only 33% identity, implicating this region in the less severe phenotype observed in *Tardbp*-null flies. More consistent with our data are reports that knockdown of TDP-43 in mammalian cell culture models can lead to loss of cell proliferation (22), inhibition of differentiation, and neuronal cell death (23).

TDP-43 Gene Expression Is Prominent in Neuroepithelium and in Central Nervous System Regions Affected in ALS and FTLD-U—The β-galactosidase reporter harbored in heterozygotic embryos and mice provides an ideal tool to examine spatial and temporal expression patterns of *Tardbp*, which should provide insight into how TDP-43 may contribute to development. At 9.5 dpc, X-gal staining was strongly detected throughout the neuroepithelium (Fig. 5, *A* and *B*), which contains neural progenitors cells that eventually form the central nervous system. Staining was also present to a lesser extent in the developing heart, first branchial arch, second branchial membrane, and somite (Fig. 5*B*). Using TDP-43 and β-galactosidase antibodies we show that the expression pattern of endogenous TDP-43 corresponds with that of the TDP-43-β-galactosidase fusion protein in the developing spinal cord of E10.5 embryos (Fig. 6*A*). X-gal staining of whole E10.5 embryos reveals prominent staining in the mid and hindbrain and in the developing spinal cord as well as the developing limbs (Fig. 6*B*). Furthermore, X-gal staining has the same pattern of expression in the developing spinal cord as seen using TDP-43 and β-galactosidase antibodies (Fig. 6*B*). Because the staining X-gal is dependent on an enzymatic reaction, the intensity of staining is greater where there is more enzyme present, unlike antibody staining. Differentiation of the spinal cord occurs at E12.5 (30), X-gal staining is detected in spinal cord progenitors and differentiated motor neurons and in the dorsal root ganglia (Fig. 6*C, panel i*). X-gal staining is also prominent in progenitors of the developing brain (Fig. 6*C, panel ii*).

In contrast to the restricted expression pattern in the developing embryos (E9.5–10.5), X-gal staining of tissues from adult *Tardbp*$^{+/-}$ mice revealed more widespread expression of TDP-43 (Fig. 7). In the brain, β-galactosidase expression was largely present in the hippocampus, cortex, and Purkinje cells of the cerebellum and the glomerular layer of the olfactory bulb (Fig. 7, *i–iv*). β-Galactosidase expression was in the gray matter of the spinal cord, with particularly intense staining in the dorsal horn (Fig. 7*v*). Staining patterns in the brain and spinal cord are consistent with *in situ* results from the Allen Brain Atlas. LacZ staining was also observed in the bronchiole of the lung, oocytes of the ovary, as well as in areas of the testes involved in spermatogenesis, cortex of the kidney, hepatocytes of the liver, and throughout the heart (Fig. 7, *vi–xi*).

Patients with ALS experience loss of motor function and have TDP-43 inclusions in the gray matter of the spinal cord, whereas patients with FTLD-U have TDP-43 inclusions in the cortex and the hippocampal regions of the brain (13). The prominent presence in adult mice of TDP-43 in these affected areas are consistent with their susceptibility to TDP-43 pathologies in humans. Considering embryonic TDP-43 expression is localized to the neuroepithelium, which contains neural progenitors that give rise to interneuron subtypes and motor neurons (31), it is conceivable that mutations or alterations in TDP-43 regulation may alter normal central nervous system development, making individuals more sensitive to TDP-43-related pathologies later in life.

Concluding Remarks—In this study we produced and characterized a null mouse model of TDP-43, and analyzed the spatial and temporal distribution patterns of TDP-43. We observed that TDP-43 is required for early embryogenesis and that TDP-43 is prominent in the neuroepithelium in developing embryos and various adult central nervous system regions afflicted in neurodegenerative disorders. Moreover, we observed that TDP-43 protein levels are developmentally regulated in postnatal brain development. These observations raise the possibility that alterations of the regulation and normal function of TDP-43 during animal development may result in the pathological degeneration that occurs in ALS and FTLD-U. This work thus provides basic information for and novel insight into understanding the developmental, physiological, and biochemical roles of TDP-43, setting up a foundation for testing if and how alteration of TDP-43 leads to neurodegenerative diseases.

REFERENCES

1. Wang, H. Y., Wang, I. F., Bose, J., and Shen, C. K. (2004) *Genomics* **83,** 130–139
2. Ayala, Y. M., Pantano, S., D'Ambrogio, A., Buratti, E., Brindisi, A., Marchetti, C., Romano, M., and Baralle, F. E. (2005) *J. Mol. Biol.* **348,** 575–588
3. Dreyfuss, G., Matunis, M. J., Piñol-Roma, S., and Burd, C. G. (1993) *Annu. Rev. Biochem.* **62,** 289–321
4. Buratti, E., and Baralle, F. E. (2008) *Front. Biosci.* **13,** 867–878
5. Ou, S. H., Wu, F., Harrich, D., García-Martínez, L. F., and Gaynor, R. B. (1995) *J. Virol.* **69,** 3584–3596
6. Buratti, E., Dörk, T., Zuccato, E., Pagani, F., Romano, M., and Baralle, F. E. (2001) *EMBO J.* **20,** 1774–1784
7. Mercado, P. A., Ayala, Y. M., Romano, M., Buratti, E., and Baralle, F. E. (2005) *Nucleic Acids Res.* **33,** 6000–6010
8. Bose, J. K., Wang, I. F., Hung, L., Tarn, W. Y., and Shen, C. K. (2008) *J. Biol. Chem.* **283,** 28852–28859
9. Strong, M. J., Volkening, K., Hammond, R., Yang, W., Strong, W., Leystra-Lantz, C., and Shoesmith, C. (2007) *Mol. Cell Neurosci.* **35,** 320–327
10. Casafont, I., Bengoechea, R., Tapia, O., Berciano, M. T., and Lafarga, M. (2009) *J. Struct. Biol.* **167,** 235–241
11. Buratti, E., Brindisi, A., Giombi, M., Tisminetzky, S., Ayala, Y. M., and Baralle, F. E. (2005) *J. Biol. Chem.* **280,** 37572–37584
12. Forman, M. S., Trojanowski, J. Q., and Lee, V. M. (2007) *Curr. Opin. Neurobiol.* **17,** 548–555
13. Neumann, M., Sampathu, D. M., Kwong, L. K., Truax, A. C., Micsenyi, M. C., Chou, T. T., Bruce, J., Schuck, T., Grossman, M., Clark, C. M., McCluskey, L. F., Miller, B. L., Masliah, E., Mackenzie, I. R., Feldman, H., Feiden, W., Kretzschmar, H. A., Trojanowski, J. Q., and Lee, V. M. (2006)

Science **314,** 130–133
14. Amador-Ortiz, C., Lin, W. L., Ahmed, Z., Personett, D., Davies, P., Duara, R., Graff-Radford, N. R., Hutton, M. L., and Dickson, D. W. (2007) *Ann. Neurol.* **61,** 435–445
15. Nakashima-Yasuda, H., Uryu, K., Robinson, J., Xie, S. X., Hurtig, H., Duda, J. E., Arnold, S. E., Siderowf, A., Grossman, M., Leverenz, J. B., Woltjer, R., Lopez, O. L., Hamilton, R., Tsuang, D. W., Galasko, D., Masliah, E., Kaye, J., Clark, C. M., Montine, T. J., Lee, V. M., and Trojanowski, J. Q. (2007) *Acta Neuropathol.* **114,** 221–229
16. Lagier-Tourenne, C., and Cleveland, D. W. (2009) *Cell* **136,** 1001–1004
17. Buratti, E., and Baralle, F. E. (2009) *Adv. Genet* **66,** 1–34
18. Igaz, L. M., Kwong, L. K., Chen-Plotkin, A., Winton, M. J., Unger, T. L., Xu, Y., Neumann, M., Trojanowski, J. Q., and Lee, V. M. (2009) *J. Biol. Chem.* **284,** 8516–8524
19. Zhang, Y. J., Xu, Y. F., Cook, C., Gendron, T. F., Roettges, P., Link, C. D., Lin, W. L., Tong, J., Castanedes-Casey, M., Ash, P., Gass, J., Rangachari, V., Buratti, E., Baralle, F., Golde, T. E., Dickson, D. W., and Petrucelli, L. (2009) *Proc. Natl. Acad. Sci. U.S.A.* **106,** 7607–7612
20. Wegorzewska, I., Bell, S., Cairns, N. J., Miller, T. M., and Baloh, R. H. (2009) *Proc. Natl. Acad. Sci. U.S.A.* **106,** 18809–18814
21. Feiguin, F., Godena, V. K., Romano, G., D'Ambrogio, A., Klima, R., and Baralle, F. E. (2009) *FEBS Lett.* **583,** 1586–1592
22. Ayala, Y. M., Misteli, T., and Baralle, F. E. (2008) *Proc. Natl. Acad. Sci. U.S.A.* **105,** 3785–3789
23. Iguchi, Y., Katsuno, M., Niwa, J., Yamada, S., Sone, J., Waza, M., Adachi, H., Tanaka, F., Nagata, K., Arimura, N., Watanabe, T., Kaibuchi, K., and Sobue, G. (2009) *J. Biol. Chem.* **284,** 22059–22066
24. Sugita, S., and Südhof, T. C. (2000) *Biochemistry* **39,** 2940–2949
25. Roche, K. W., and Huganir, R. L. (1995) *Neuroscience* **69,** 383–393
26. Pulipparacharuvil, S., Renthal, W., Hale, C. F., Taniguchi, M., Xiao, G., Kumar, A., Russo, S. J., Sikder, D., Dewey, C. M., Davis, M. M., Greengard, P., Nairn, A. C., Nestler, E. J., and Cowan, C. W. (2008) *Neuron* **59,** 621–633
27. Nikolaev, A., McLaughlin, T., O'Leary, D. D., and Tessier-Lavigne, M. (2009) *Nature* **457,** 981–989
28. Stoecklin, G., Mayo, T., and Anderson, P. (2006) *EMBO Rep.* **7,** 72–77
29. Wu, L. S., Cheng, W. C., Hou, S. C., Yan, Y. T., Jiang, S. T., and Shen, C. K. (2009) *Genesis* **48,** 56–62
30. Helms, A. W., and Johnson, J. E. (2003) *Curr. Opin. Neurobiol.* **13,** 42–49
31. Rowitch, D. H. (2004) *Nat. Rev. Neurosci.* **5,** 409–419